Additive Manufacturing Letters 6 (2023) 100146

Contents lists available at ScienceDirect

Additive Manufacturing Letters

journal homepage: www.elsevier.com/locate/addlet

Short Communication

Bend-Forming: A CNC deformation process for fabricating 3D wireframe structures

Harsh G. Bhundiya, Zachary C. Cordero*

Aeronautics and Astronautics, Massachusetts Institute of Technology, Cambridge, MA 02139, United States

ARTICLE INFO

Keywords:
Wireframe structures
Path planning
Additive manufacturing
Deformation processing

ABSTRACT

This paper presents a computer numerical control (CNC) deformation process, termed Bend-Forming, for fabricating 3D wireframe structures. The process relies on the combination of CNC wire bending with mechanical joints to construct reticulated structures from wire feedstock. A key component of the process is a path planning framework which uses Euler paths and geometrical computations to derive fabrication instructions for arbitrary 3D wireframe geometries. We demonstrate the process by fabricating exemplary structures on the order of 1 m, including reticulated columns, shells, and trusses, with rapid build times compared to other additive manufacturing techniques. The structures fabricated herein contain defects which result in residual stress and imperfect geometries. To determine the tolerances needed to fabricate accurate structures, we develop a model of error stack-up for Bend-Forming, using fabrication defects in feed length, bend and rotate angle, and strut curvature. We find that for tetrahedral trusses fabricated with Bend-Forming, defects in feed length and strut curvature have a large effect on the surface precision and stiffness of the truss, respectively, and are thus important tolerances to control to achieve structural performance metrics. Overall, Bend-Forming is a versatile and low-power process that is well suited for a wide-range of applications, from rapid prototyping of wireframe structures to in-space manufacturing.

1. Introduction

Computer numerical control (CNC) deformation processes which plastically deform metallic feedstock have attracted interest due to their ability to form near-net shapes without complex tooling, thereby offering speed and cost improvements over conventional manufacturing processes. Deformation processes are also attractive for applications where power is limited, given their lower specific energy consumption (<1 MJ/kg) as compared to other melt-based and extrusion processes which require melting of feedstock (5–10 MJ/kg) [1]. One deformation process of particular interest for fabricating lightweight structures is the CNC bending of wire, tubes, and profiles, which has been developed over decades and routinely used in manufacturing industries [2–4]. Many variations of this process have been developed for fabricating 2D and 3D bent profiles, including draw bending [5,6], shear bending [7], MOS tube bending [8], dieless U-bending [9], TSS profile bending [10], and HexaBend profile bending [11]. Additionally, smart CNC bending processes with increased accuracy have been developed by using heated feedstock and dies [12], simultaneous hot bending and quenching [13], and even closed-loop control [14]. These various processes have enabled the flexible forming of 3D bent profiles for both large-scale and small-scale applications. For instance on the small scale, CNC wire bending has been used to manufacture wire sculptures [15], kinetic wire characters [16], compliant mechanisms [17], and braces for orthodontics [18]. Nonetheless, using CNC wire bending to fabricate 3D wireframe structures from continuous feedstock has not been considered, and a general framework for fabricating arbitrarily complex 3D geometries has not been developed, restricting potential applications of the process. The primary constraint for fabrication with CNC wire bending is that the structure be made from continuous feedstock, which offers a unique path planning challenge: How to fabricate a given 3D wireframe structure by deforming only one strand of feedstock? Additionally, for large structures, how do errors at each fabrication step propagate and affect accuracy of the final geometry?

In this paper, we tackle these questions by developing a process termed Bend-Forming, which incorporates CNC wire bending with mechanical joints to fabricate 3D wireframe structures. At the crux of the process is a path planning framework (Section 2) which uses Euler paths and geometrical computations to convert a 3D wireframe structure into fabrication instructions for a CNC wire bender. Using this framework, we fabricate exemplary structures previously not possible with CNC wire bending (Section 3). Additionally, to enable fabrication of accurate structures with Bend-Forming, we analyze the error stack-up of the process based on the tolerances of each fabrication step (Section 4).

* Corresponding author.
E-mail address: zcordero@mit.edu (Z.C. Cordero).

https://doi.org/10.1016/j.addlet.2023.100146
Received 18 January 2023; Received in revised form 2 May 2023; Accepted 7 May 2023

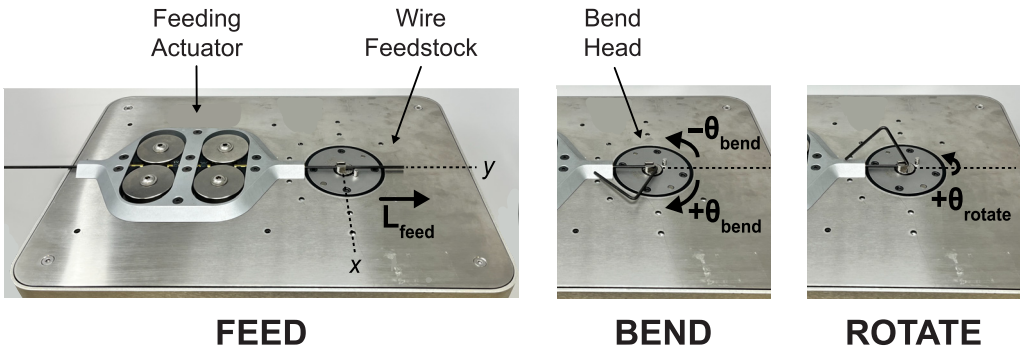

Fig. 1. The three degrees of freedom (DOFs) of a CNC wire bender: feed, bend, rotate. The machine feeds along the wire axis (L_{feed}), bends clockwise or counter-clockwise in the xy-plane ($\pm\theta_{bend}$), and rotates the wire out-of-plane about the feeding axis ($\pm\theta_{rotate}$). To avoid self-collision, the bend angle is typically restricted to $0° < |\theta_{bend}| < 180°$ This illustration is based off the D.I. Wire Pro machine [6].

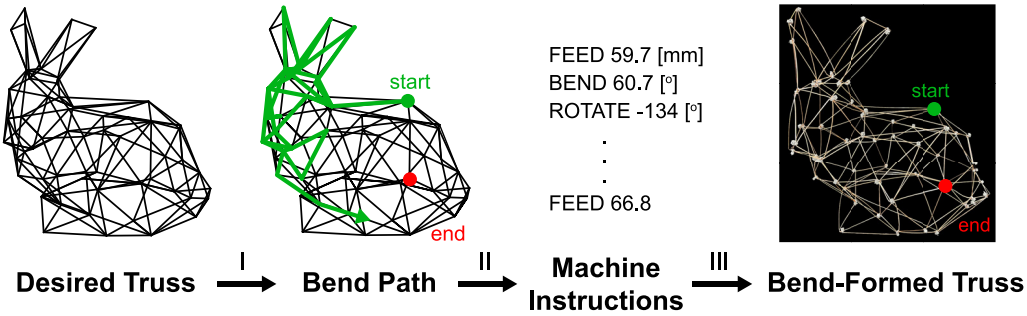

Fig. 2. Bend-Forming fabrication process. **(I)** A bend path is found which continuously traverses each edge of the desired wireframe geometry. The green and red dots indicate the path's start and end points. **(II)** The bend path is converted into a list of machine instructions. **(III)** The machine instructions are implemented on a CNC wire bender and the neighboring edges are joined at each node. The result is a stiff structure made from a continuous strand of feedstock.

With a case study on tetrahedral trusses, we highlight how structural performance metrics can be achieved with Bend-Formed structures, by keeping the fabrication tolerances within specified ranges. Note the software tools developed for this work, i.e. for the fabrication and accuracy modeling of Bend-Formed structures, are publicly available at [19].

2. Bend-Forming process

Bend-Forming combines CNC wire bending with mechanical joints to form wire feedstock into 3D reticulated structures. The unit process is illustrated in Fig. 1, which depicts a CNC wire bender plastically deforming a straight wire via the three degrees of freedom (DOFs) of the machine: feed, bend, rotate. Note that these elementary steps are typical for all CNC wire benders. To fabricate larger wireframe structures, a sequence of feed, bend, and rotate instructions is prescribed to the machine, such that the bends serve as nodes and the straight sections serve as struts. A joining method is then used to connect the neighboring edges at each node. The final result is a stiff structure made from a continuous strand of wire feedstock. By combining CNC wire bending with mechanical joints in this way, Bend-Forming can fabricate lightweight yet stiff wireframe structures from ductile feedstock.

Below we summarize the path planning framework for fabricating arbitrary wireframe geometries with Bend-Forming. The process consists of three steps, as depicted in Fig. 2. The first step is to find the shortest bend path which continuously traverses each edge of the desired geometry. Graph theory is used to find such paths for any 2D or 3D geometry, as described in Section 2.1. The second step is to convert the bend path into machine instructions, namely a list of feed, bend, and rotate steps which can be inputted into the CNC wire bender for fabrication. A geometric algorithm which uses nodal coordinates is implemented in this step to generate the machine instructions, as described in Section 2.2. The final step is to input the machine instructions into a CNC wire bender and fabricate the desired structure, using the joining methods described in Section 2.3.

2.1. Finding bend paths

The first step of the Bend-Forming process is to find a bend path which traverses the desired wireframe geometry, such that it can be fabricated from continuous feedstock. To minimize mass of the structure, we seek bend paths with shortest length. This problem is a version of the route inspection problem, which seeks the shortest closed path which visits each edge of a graph [20]. As any wireframe geometry can be represented as a graph with nodes and edges, the algorithm which solves this problem is directly applicable to finding bend paths for Bend-Formed structures. Thus, here we describe the route inspection algorithm, but specifically applied to Bend-Forming. Note that this methodology does not consider any plasticity or specific tooling knowledge to compute bend paths; it solely uses the desired wireframe geometry represented as a graph. This approach is similar to that presented in [21], where the route inspection algorithm is used to find optimal tool paths for fused deposition modeling (FDM) of lattices.

The goal of the route inspection algorithm is to compute a continuous bend path for an arbitrary wireframe geometry. Recall Euler's theorem, which holds that there exists a closed path which traverses each edge of a graph if and only if there are no more than two nodes with an odd number of connections [20]. Therefore to find continuous bend paths (also called Euler paths), we first check whether the desired geometry satisfies this condition. If not, we add the minimum number of doubled edges until this condition is satisfied and the graph is made Eulerian. Physically, these edges represent doubled struts which are added to the wireframe structure in order to fabricate it from a continuous strand of feedstock. Once these struts are added, we find a bend path which fully traverses the geometry, using the algorithm of Hierholzer [22].

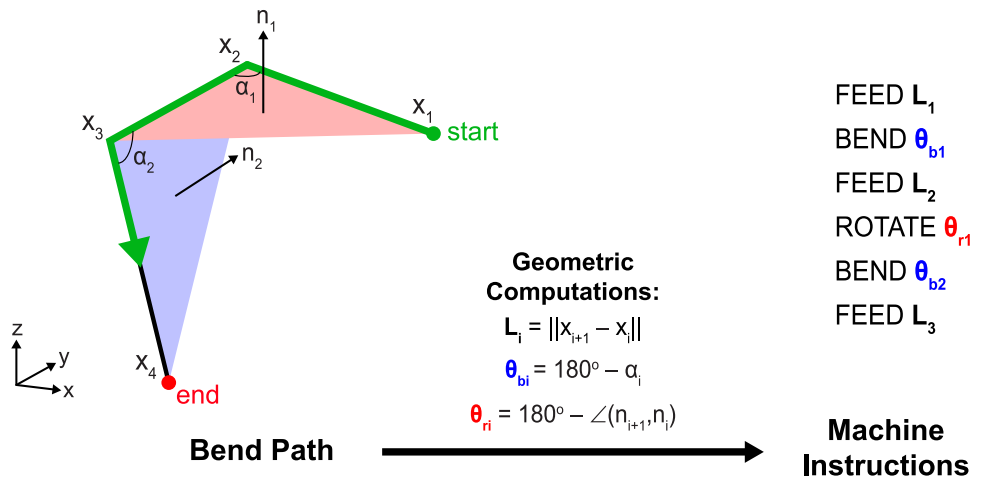

Fig. 3. Converting a 3D bend path of four nodes (x_1-x_4) into machine instructions for a CNC wire bender. The feed length (L_i) is computed via the Euclidean distance between subsequent nodes; the bend angle (θ_{bi}) via the angle between every three nodes; and the rotation angle (θ_{ri}) via normal vectors to every three nodes. The green line indicates the progression of the bend path.

The pseudocode for these two steps of the route inspection algorithm (i.e. adding doubled struts and finding a bend path) are provided in the Supplementary Material. The bend path found by this algorithm is not unique as many exist for the same geometry. Each bend path, however, is guaranteed to have the shortest length which traverses each edge of the wireframe geometry exactly once. In terms of complexity, the most efficient implementation of the algorithm runs in $O(V^3)$ time, where V is the number of nodes in the geometry [20].

2.2. Converting to machine instructions

Once a bend path is found for the desired geometry, the next step is to convert the path into instructions for a CNC wire bender. To do so, we implement an algorithm which converts a list of nodal coordinates which constitute the bend path into a series of feed, bend, and rotate instructions for the CNC wire bender. For these computations, we assume that each feed length, bend angle, and rotate angle will be perfectly implemented by the machine. In reality, the tolerances of the machine as well as the springback and curvature of the feedstock affect each fabrication step and lead to geometrical errors which accumulate for larger structures, as discussed further in Section 4. To some extent, these factors can be corrected for when generating the machine instructions, for instance, by compensating for springback and adjusting feed lengths using the diameter of the wire and bend head. However, here we do not consider these adjustments and instead present a purely geometrical algorithm for generating the machine instructions for a typical CNC bending machine. The output of this algorithm may subsequently be combined with springback compensation to generate accurate machine instructions for specific machines. This methodology is similar to that used for commercially-available tube benders [23] and dental wire benders [24].

The key computations of the algorithm for calculating machine instructions are depicted in Fig. 3 for a simple 3D bend path of four nodes. The feed length is calculated as the Euclidean distance between subsequent nodes; the bend angle as the supplement of the angle between every three nodes; and the rotate angle as the supplement of the angle between planes formed by every three nodes. By using the order of nodal coordinates and computing the distances and angles between subsequent nodes in this way, the algorithm converts a bend path into fabrication instructions for a CNC wire bender. The detailed pseudocode for this algorithm is provided in the Supplementary Material, including a description of edge cases such as doubled struts and collinear nodes.

Table 1
Fabrication details of the exemplary Bend-Formed structures shown in Fig. 4. Note that the listed mass includes both the wire and the joints.

Prototype	Feedstock Length (m)	Bends	Mass (g)	Embodied Energy (kJ)	Theoretical Build Time (min)
Tetrahedral Truss	5.6	79	29	9.5	6
Utah Teapot	10.6	216	54	18	12
Stanford Bunny	11.9	176	60	20	13
Curved Gridshell	28.5	241	183	60	40
Isogrid Column	27.4	271	218	72	48

2.3. Joining

The algorithms presented in Sections 2.1 and 2.2 convert a desired 3D wireframe geometry into fabrication instructions for a CNC wire bender. The final fabrication step of Bend-Forming is to implement the machine instructions and attach joints at each node to construct a stiff structure. Various solid-state and mechanical methods may be used to create the joints. Here we highlight two such joining methods which are compatible with the Bend-Forming process: interference snap-fit joints and solder joints. The interference snap-fit joints contain two parts which snap together at the node with interfering pins (as further described in [25]), while the solder joints strengthen the nodes with a filler metal. For the prototypes presented herein, such joints were manually attached to the structure after fabrication with a CNC wire bender. To enable robotic construction of stiff structures, joint application should be integrated with the CNC process to incrementally join nodes during Bend-Forming.

3. Exemplary structures

Using the fabrication and joining processes outlined in Section 2, Fig. 4 presents photos of exemplary structures fabricated with Bend-Forming, with dimensions on the order of 1 m. Here the feedstock was 1-mm diameter steel wire and bending was performed with the D.I. Wire Pro machine after calibrating for material springback [6]. Snap-fit joints, solder joints, and zipties were used as the joints, as shown in the inset images. The snap-fit joints were 3D printed on a FormLabs SLA printer [26] and attached to the structure after fabrication. For each prototype, Table 1 lists the total length of feedstock, the number of bends, and the mass. Additionally, Table 1 lists the embodied energy of each prototype,

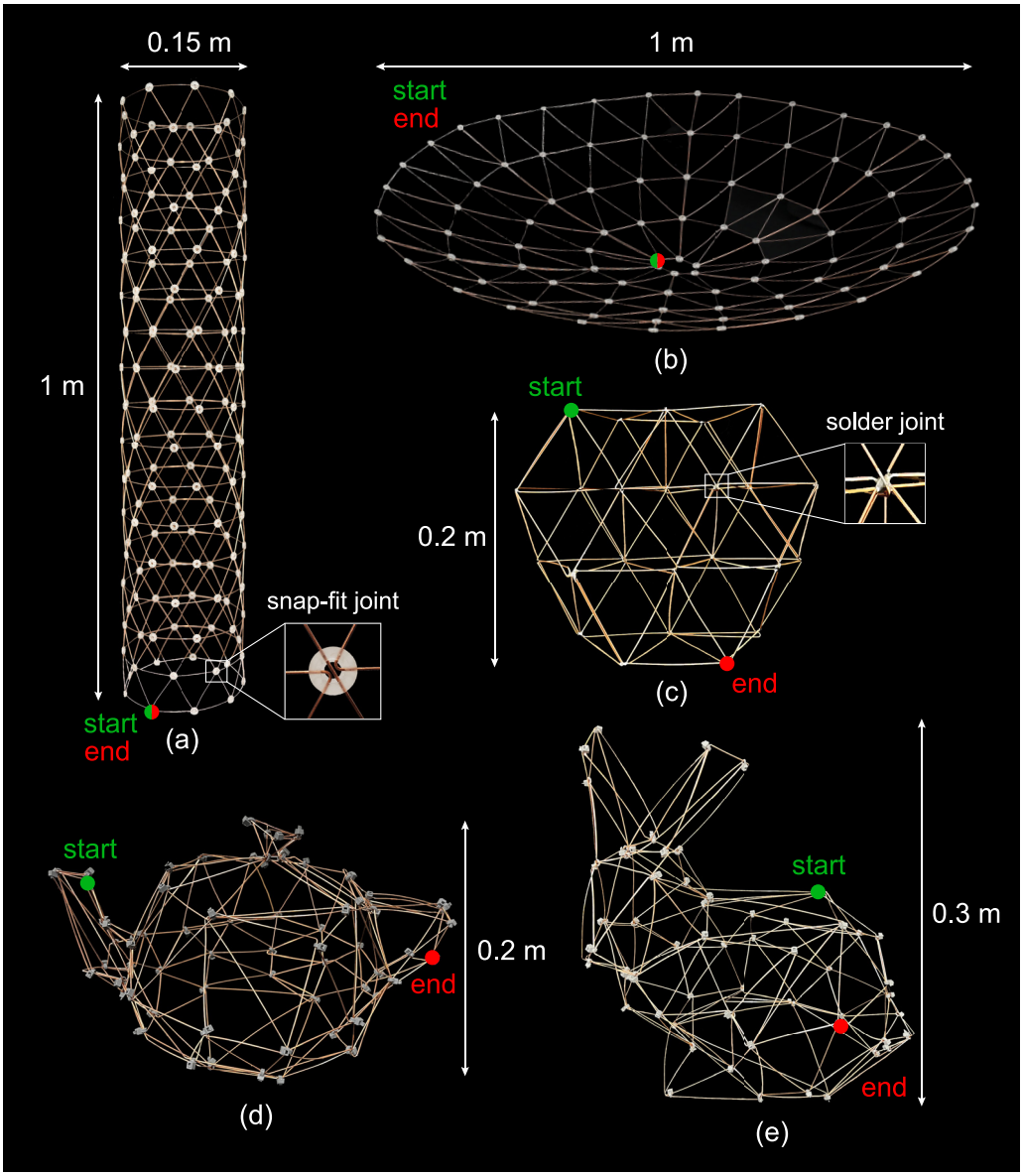

Fig. 4. Photos of exemplary 3D wireframe structures fabricated with Bend-Forming: (a) isogrid column, (b) curved gridshell, (c) tetrahedral truss, (d) Utah teapot, and (e) Stanford bunny. Each prototype is made from a single, continuous steel wire via a desktop CNC wire bending machine [6]. The green and red dots indicate the start and end points of the wire. The nodes consist of zipties, solder joints, and plastic snap-fit joints which lock together with interfering pins (see insets).

calculated using a specific energy consumption of 0.33 MJ/kg for a typical deformation process [1], and the theoretical build time, calculated using a power draw of 25 W for a typical CNC wire bender [6]. Further details regarding the geometry, bend path, and fabrication of each structure are provided in the Supplementary Material.

The prototypes of Fig. 4 demonstrate that while the Bend-Forming process relies on only a few DOFs, it can fabricate complex 3D wireframe structures. The theoretical build times also demonstrate the rapid fabrication possible with Bend-Forming, given its relatively low specific energy consumption compared to additive manufacturing techniques which require melting of feedstock.

4. Accuracy model of Bend-Forming

Compared to their perfect geometries, the Bend-Formed prototypes presented in Fig. 4 have geometrical defects arising from their fabrication process. These defects result from various sources, e.g., incomplete compensation for material springback, incomplete straightening of feedstock, and angular errors of the bending mechanism. As Bend-Formed structures are fabricated from a continuous strand of feedstock, these errors affect each fabrication step and accumulate for large structures. Hence to fabricate accurate structures, an understanding is needed of the error stack-up during Bend-Forming and its effect on the final geometry.

Here we present an accuracy model which allows for an estimation of the accuracy of Bend-Formed structures given fabrication tolerances of the CNC wire bender. An overview of this modeling framework is presented in Fig. 5. We consider three specific fabrication defects: feed length error (δ_L), angular error (δ_θ), and strut curvature (δ_κ). With these fabrication defects and a specific wireframe geometry, we use a kinematic model to replicate the imperfect fabrication of the structure. We then implement a finite element model to close the fabrication defects, which physically represents joint attachment at each node. The result of these two steps is the residual stress distribution and deformed geometry of an imperfect wireframe structure fabricated with Bend-Forming. This imperfect structure can then be used to conduct trade studies and understand how its performance varies with fabrication defects. Practi-

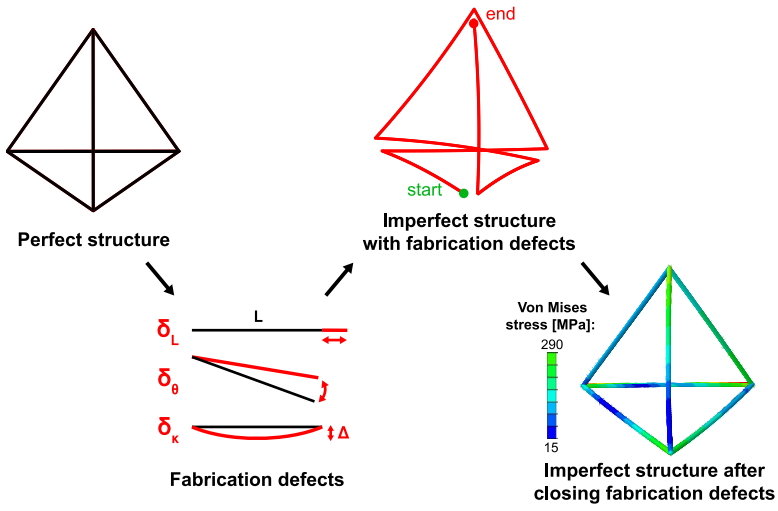

Fig. 5. Modeling framework for estimating the accuracy of Bend-Formed structures. An imperfect structure is modeled by replicating fabrication with defects: feed length error (δ_L), angular error (δ_θ), and strut curvature ($\delta_\kappa = \Delta/L$). The defects are then closed by aligning adjacent nodes in a finite element model. The resulting imperfect structure has residual stress and deformations not present in the perfect structure. The tetrahedron shown here has sidelength $L = 50$ mm and fabrication defects $[\delta_L, \delta_\theta, \delta_\kappa] = [-1\text{ mm}, -3°, 2\%]$.

cally, it can also be used to derive ranges of the fabrication tolerances to achieve specific performance metrics with Bend-Formed structures.

4.1. Kinematic model of imperfect fabrication

To compute an imperfect Bend-Formed geometry with fabrication defects, we implement a kinematic model of error stack-up. Specifically, we add three types of fabrication defects to the bend path of a given wireframe structure. The first defect is an absolute offset in feed length (δ_L), resulting from tolerances of the feeding mechanism in a typical CNC wire bender ($|\delta_L| \sim 0.1$mm for the D.I. Wire Pro [6]). The second defect is an offset in the bend and rotate angles (δ_θ), resulting from incomplete compensation for material springback during bending operations and torsion during rotate operations ($|\delta_\theta| \sim 0.5°$-$1.0°$). Many CNC wire/tube benders can actually compensate for the rotate error with sufficient distance between the feedstock spool and bend head to minimize the torsional shear strain (e.g. with an accumulator [27]); however here we assume a worst-case fabrication scenario in which the angular error is identical for all bend and rotate angles. This conservative assumption may not be valid for Bend-Formed geometries with a small number of fabrication steps but become valid for larger structures, for which the rotate error may be difficult to compensate for due to the large inertia of the fabricated structure. The third defect corresponds to nonzero strut curvature (δ_κ), resulting from the incomplete straightening of the feedstock as it is drawn from the spool, which imparts both cast and helix curvatures ($\delta_\kappa \sim 1$–5%). Here δ_κ is defined as the ratio of the maximum transverse offset (Δ) of a symmetric, circular arc between strut nodes to the strut length (L). To account for both systematic and random errors, these three fabrication defects are expressed as the sum of a constant C_i and a normal distribution $N(0, \sigma_i^2)$ with zero mean and standard deviation σ_i, where $i = \{L, \theta, \kappa\}$:

$$\delta_i = C_i + N\left(0, \sigma_i^2\right). \tag{1}$$

For each strut in the perfect geometry, Eq. (1) is used to compute an error in its length (δ_L), bend/rotate angle (δ_θ), and curvature (δ_κ). Here the constant term C_i represents a systematic error that is constant for each strut, while the standard deviation σ_i represents a random error that varies for each strut.

To model the accumulation of these errors during Bend-Forming, we incorporate them into the bend path of the perfect structure and use homogeneous transformation matrices (HTMs) [28,29] to replicate fabrication of the imperfect structure. Specifically, we add the feed length and angular errors (δ_L, δ_θ) to each feed and bend/rotate step of the bend path, respectively, and calculate the nodal coordinates of the imperfect geometry by modeling the fabrication as a combination of translations and rotations. Then we add strut curvature (δ_κ) by fitting a symmetric, circular arc between the start and end points of each strut and assuming a random curvature direction perpendicular to the strut axis. The resulting imperfect structure contains geometrical defects (as depicted in Fig. 5) and represents the accumulation of error at the end of fabrication. Note that this kinematic model does not consider the residual stresses from the bending operations or how the defects change during fabrication, which may affect the predicted imperfect geometry. See Appendix A for a detailed mathematical description of this kinematic model.

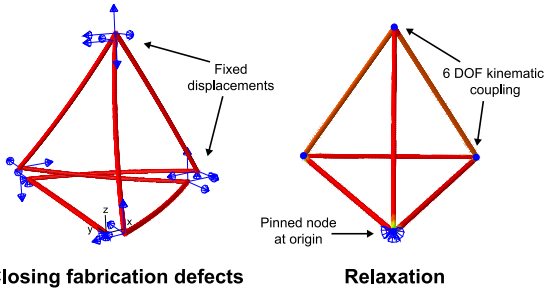

Fig. 6. Simulation of closing fabrication defects. The nodes of the imperfect structure are aligned with the perfect structure via fixed displacements, after which the displacements are removed and the structure is allowed to move freely. The resulting structure contains residual stress and a deformed geometry which represents the final shape of the Bend-Formed structure.

4.2. Simulation of closing fabrication defects

After calculating the geometry of the imperfect structure, we close the fabrication defects to calculate the resulting residual stress and deformed geometry which represent the final shape of the Bend-Formed structure. Physically, this step corresponds to the fabrication step of attaching joints at each node (cf. Section 2.3). Here we simulate this step with a finite element model, by meshing the imperfect geometry with linear beam elements (B31 in Abaqus) and implementing two analysis steps, as illustrated in Fig. 6. In the first step, displacements are simultaneously applied to all nodes of the imperfect geometry to align them

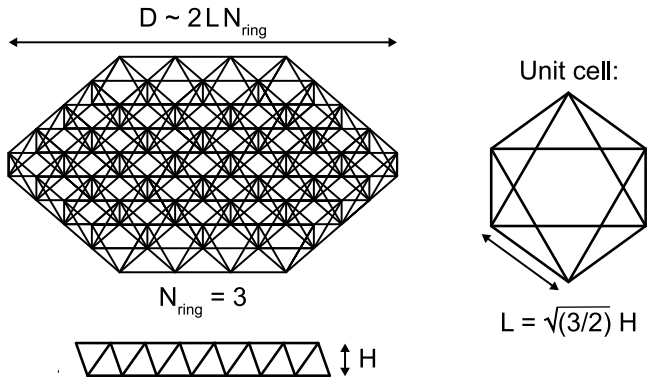

Fig. 7. Tetrahedral truss, parametrized by its depth H and number of rings N_{ring}. All struts have equal length L.

with the perfect structure. This brings the strut axes together at each node, effectively closing the geometrical defects from imperfect fabrication. The imperfect geometry used for this step is the output of the kinematic model, which solely considers the fabrication path and geometrical defects. Hence we do not include any residual stresses from the bending operations, which may affect the closing of the defects as described here. In the second step, the displacements are removed and the structure is allowed to move freely, while adjacent nodes are constrained to move together and one node is pinned at the origin. This replicates the attachment of joints to the structure and subsequent relaxation of stress. We implement this relax step with a user-defined subroutine in Abaqus which kinematically couples all six DOFs of adjacent nodes. The result of these two analysis steps (i.e. closing fabrication defects and relaxation) is the residual stress and deformed geometry of the imperfect Bend-Formed structure.

Once the imperfect Bend-Formed structure has been computed, it can be compared to the perfect structure to determine its accuracy and to characterize performance, for example by calculating precision and stiffness metrics as presented in Section 4.3. This analysis can then guide the selection of appropriate ranges for fabrication tolerances. Note that due to the perfect alignment of struts at the nodes, this model assumes perfect joint attachment and does not consider any joint assembly errors, which may result in additional imperfections to the final structure. Additionally, due to the kinematic coupling of adjacent nodes, this model assumes perfect load transfer at the joints, yielding a conservative estimate of the residual stress.

4.3. Case study: Bend-Formed tetrahedral truss

Using the accuracy model presented above, we present a case study which highlights the effect of fabrication defects on the performance of a Bend-Formed tetrahedral truss. This truss geometry (fabricated in Fig. 4) consists of rings of a hexagonal unit cell with equal-length struts and is parametrized by its depth H and number of rings N_{ring}, as illustrated in Fig. 7. The tetrahedral truss is used commonly in load-bearing applications as a lightweight yet stiff support structure [30].

Here we conduct trade studies to illustrate how the fabrication errors of Bend-Forming affect the structural performance of the tetrahedral truss. We first investigate how random feed length and angular errors affect the surface precision and residual stress of the truss. To do so, we use the framework of Sections 4.1 and 4.2 to model various imperfect tetrahedral trusses fabricated with Bend-Forming, with random defects in either feed length ($\overline{\sigma_L}$) or bend/rotate angle ($\overline{\sigma_\theta}$). For nondimensionalization, the feed length standard deviation is expressed as $\overline{\sigma_L} = \sigma_L/L$ using the strut length L; and the angular standard deviation as $\overline{\sigma_\theta}$ in radians. For each imperfect structure modeled with these errors, we compute the RMS surface error (w_{RMS}) and the RMS residual axial load (P_{RMS}), two parameters which represent the surface precision and residual stress of the tetrahedral truss. The surface error is calculated as the RMS deviation from best-fit planes to the nodes of the imperfect truss; and the residual axial load as the RMS axial force of all beam elements in the model. These parameters are then nondimensionalized as

$$\overline{w_{\text{RMS}}} = \frac{w_{\text{RMS}}}{D\bar{\sigma}}, \tag{2}$$

$$\overline{P_{\text{RMS}}} = \frac{P_{\text{RMS}}}{EA\bar{\sigma}}, \tag{3}$$

using the diameter D, the standard deviations of the random errors $\bar{\sigma} = \overline{\sigma_L}, \overline{\sigma_\theta}$, and the strut axial stiffness EA (similar to the analysis in [31]). Once nondimensionalized, these parameters are plotted in Fig. 8 against the number of rings N_{ring} for tetrahedral trusses of various size.

Each datapoint in Fig. 8 represents the average of five simulations of randomly imperfect Bend-Formed trusses made from 1-mm diameter steel wire ($E = 200$ GPa, $\nu = 0.29$), with depth $H = 50$ mm, number of rings N_{ring}, and random feed length and angular errors with standard deviation $\overline{\sigma_L} = \overline{\sigma_\theta} = 3 \times 10^{-3}$. Overlaid on this plot are analytical values from previous continuum analyses [32–34], which model the effect of random feed length errors on the RMS surface error and RMS residual axial load of tetrahedral trusses:

$$\overline{w_{\text{RMS}}} \approx 0.146, \tag{4}$$

$$\overline{P_{\text{RMS}}} = 1/\sqrt{3}. \tag{5}$$

Note that for our simulated trusses with random feed length error, a slight nonzero strut curvature between $\delta_\kappa = 0$–3% is included to enable the finite element solver to close fabrication defects past the buckling of individual struts. For these simulations, a corresponding knockdown in axial stiffness is used when nondimensionalizing the RMS axial force, given by [35]

$$\frac{EA^*}{EA} = \left(1 + \frac{1}{2}\left(\frac{\delta_\kappa L}{r_g}\right)^2\right)^{-1}, \tag{6}$$

where L is the strut length and r_g the radius of gyration of the strut cross section, both of which are held constant for all trusses.

The results of Fig. 8 show that random feed length errors have a greater effect on the RMS surface error and RMS residual axial load of Bend-Formed tetrahedral trusses than angular errors. This is a consequence of the larger stresses which develop in the struts during closing of the random feed length errors. Hence limiting the feed length errors is important for achieving structural performance metrics with Bend-Forming. At the same time, the angular errors do affect the geometry of the imperfect structure and should therefore be limited by the reach of the joining method used with Bend-Forming, i.e. to ensure all nodes of the imperfect geometry remain within reach to close fabrication defects.

The results of Fig. 8 also show that the effect of random feed length errors is well-approximated by the continuum analysis of Eqs. (4), (5). Hence these equations can be used to calculate the required range of feed length tolerances to achieve performance metrics. For example, consider the application of Bend-Forming a truss support structure for a large-diameter antenna in space (e.g. $D = 50$ m, $H = 50$ mm). Given a surface error requirement of $w_{\text{RMS}} < 1$ mm and residual axial load requirement of $P_{\text{RMS}} < 5$ N, Eqs. (4), (5) suggest that Bend-Forming such a tetrahedral truss from 1-mm diameter steel wire requires a feed length standard deviation of $\sigma_L \leq 4$ μm. Achieving this tolerance would require an extremely precise feeding mechanism, given the $\sigma_L \sim 0.1$mm tolerance of current desktop CNC wire benders [6].

We next assess the effect of strut curvature on the stiffness of Bend-Formed tetrahedral trusses, again using the modeling framework of Sections 4.1 and 4.2. Specifically we compute the free-free fundamental natural frequency (f_0) of imperfect tetrahedral trusses of various size with various strut curvatures (δ_κ), as plotted in Fig. 9. Each datapoint in Fig. 9 represents the average of five simulations of randomly imperfect Bend-Formed trusses made from 1-mm diameter steel wire ($E = 200$

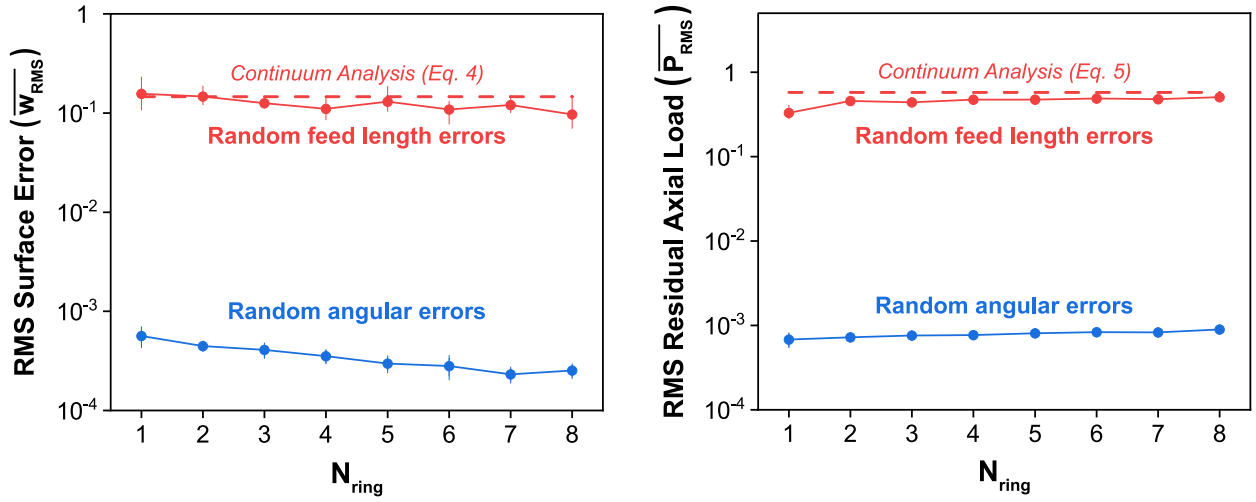

Fig. 8. Effect of random feed length and angular errors on the nondimensional RMS surface error ($\overline{w_{RMS}}$) and RMS residual axial load ($\overline{P_{RMS}}$) of Bend-Formed tetrahedral trusses.

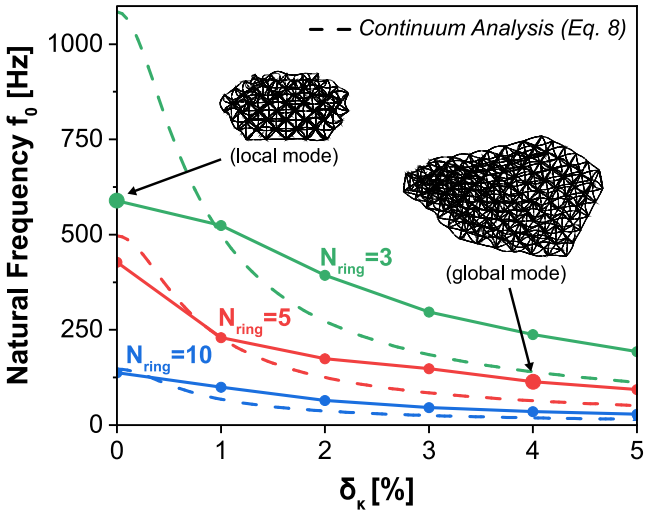

Fig. 9. Effect of strut curvature (δ_κ) on the free-free fundamental natural frequency (f_0) of Bend-Formed tetrahedral trusses. Note the transition from local to global mode shapes for larger-diameter trusses.

GPa, $\nu = 0.29$, $\rho = 7800\ \mathrm{kg/m^3}$), with depth $H = 50$ mm, number of rings N_{ring}, and constant strut curvature between $\delta_\kappa = 0$–5%. Overlaid on this plot are analytical expressions derived by combining the knockdown in strut axial stiffness from Eq. 6 with the natural frequency of a tetrahedral truss modeled as a thin plate [36,37], given by

$$f_0 = \frac{\kappa}{2\pi D}\sqrt{\frac{E^*}{\rho}}. \tag{7}$$

Here D is the truss diameter, E^* and ρ the strut Young's modulus and density, and κ a constant which varies with diameter. Substituting Eq. (6) into Eq. (7), we obtain the following relationship between natural frequency (f_0) and strut curvature (δ_κ) for a tetrahedral truss modeled as a continuum:

$$f_0 = \frac{\kappa}{2\pi D}\sqrt{\frac{E}{\rho}\left(1+\frac{1}{2}\left(\frac{\delta_\kappa L}{r_g}\right)^2\right)^{-1}}. \tag{8}$$

This expression is overlaid in Fig. 9 with simulation results for tetrahedral trusses of various size. Note that the strut length L, radius of gyration r_g, density ρ, and Young's modulus E are kept constant for all trusses.

The results of Fig. 9 show that nonzero strut curvature causes a significant decrease in natural frequency and hence stiffness of Bend-Formed tetrahedral trusses. For large trusses, this trend is approximated by the continuum analysis of Eq. (8), which assumes a global saddle mode shape and a knockdown in truss stiffness due to the decreased axial stiffness of each strut. However for smaller trusses (e.g. $N_{\mathrm{ring}} = 3$), there are discrepancies due to the presence of local mode shapes which have a lower natural frequency than the global mode shape. Nonetheless, all trusses exhibit a decrease in natural frequency with increasing strut curvature, and Eq. (8) provides a conservative estimate of this dependence. For example, consider again the application of Bend-Forming a truss support structure for a large-diameter antenna in space (e.g. $D = 50$ m, $H = 50$ mm). Eq. (8) suggests that for such a truss made from 1-mm diameter steel wire, a strut curvature of $\delta_\kappa \geq 1\%$ will result in more than a 50% decrease in natural frequency. This can be troublesome for avoiding control-structure interaction on orbit; hence limiting strut curvature during fabrication is important for achieving stiffness metrics with Bend-Forming.

5. Summary and outlook

This paper presented a CNC deformation process, termed Bend-Forming, for fabricating 3D wireframe structures by deforming a single strand of feedstock. The key novelty of Bend-Forming over previous work on CNC wire bending is a path planning framework which converts arbitrary 3D wireframe geometries into fabrication instructions for a CNC wire bender, via Euler paths and geometrical computations. This framework computes a random bend path for a desired geometry through the route inspection algorithm and converts it into machine instructions, without any knowledge regarding plasticity or the specific tooling. Here we demonstrated this framework by fabricating exemplary 3D wireframe structures, including an isogrid column, curved gridshell, and Stanford bunny. Additionally, to understand the accuracy of structures fabricated with Bend-Forming, we developed an accuracy model which provides estimates of residual stress and deformed geometry from the tolerances of the fabrication process itself. This model uses a purely geometric analysis to incorporate normally distributed feed length errors, angular errors, and strut curvatures; uses a worst-case assumption that bend and rotate errors are identical; and assumes perfect alignment of nodes to estimate the residual stress after joint attachment. As illustrated with a case study on tetrahedral trusses, this model can be used to

derive necessary fabrication tolerances to achieve precision and stiffness metrics with Bend-Formed structures.

As a method for fabricating 3D wireframe structures of arbitrary shape and size, Bend-Forming enables various small and large-scale applications. On the small scale, Bend-Forming can improve the rapid prototyping of truss structures by enabling fabrication of complex geometries with CNC wire bending. On the large scale, Bend-Forming can enable fabrication of structures with a high compaction ratio. For instance, one potential application is the in-space manufacturing of truss structures [1], which require a high compaction ratio due to the volume constraints of the rocket fairing. Bend-Forming could eliminate such constraints by enabling the construction of large-volume structures on orbit from a relatively small volume of spooled feedstock material. Another potential large-scale application is the fabrication of space frames for terrestrial infrastructure.

To enable these various applications, future work is needed to refine the Bend-Forming process. One key area of improvement is to automate the joint attachment during fabrication. For all the prototypes presented in this paper, the joints were manually attached to the structure after fabrication; whereas for robotic fabrication, a system for automatic joint attachment would need to be integrated with the process. A second area of improvement is to select optimized bend paths suited to fabrication. The challenge (and opportunity) of Bend-Forming is that many bend paths can be used to fabricate the same wireframe geometry, hence selecting bend paths which achieve minimal collision or maximize the natural frequency of intermediate structures can significantly improve the fabrication process. Another area of improvement, particularly for fabricating large structures, is to increase the accuracy of the Bend-Forming process. While the accuracy model presented in this paper provides guidelines for estimating the required fabrication tolerances, our model can be improved in several ways. In particular, the conservative assumption of identical bend and rotate errors can be improved for the specific tooling used, and the residual stresses from bending operations can be incorporated before estimating the residual stresses from closing fabrication defects. Practically, methods such as the *in-situ* correction of defects with closed-loop control can also greatly improve the accuracy of Bend-Formed structures. Finally, novel feedstock materials can achieve Bend-Formed structures with higher specific stiffness. While the plastic deformation of the process restricts potential feedstock to ductile materials, novel material architectures (e.g. with functionally-graded ductility) should be developed which are both amenable to Bend-Forming and result in stiffer struts.

Declaration of Competing Interest

The authors declare the following financial interests/personal relationships which may be considered as potential competing interests: Harsh Bhundiya and Zachary Cordero have the patent “Computer numerical control (CNC) deformation process for forming 3D wireframe structures” pending to USPTO.

Data availability

Data will be made available on request.

Acknowledgments

The authors would like to acknowledge funding from the MIT Lincoln Laboratory Advanced Concepts Committee and the Northrop Grumman Corporation. HGB was also supported by the MIT Mathworks fellowship. Special thanks to Sonny Jeon, Mark Silver, and Prof. Fabien Royer for discussions regarding the accuracy model and to Kaleb Overby, Brennan Hoppa, Jack Ansley, and Elizabeth Zhu for their help in fabrication of the wireframe structures.

Supplementary materials

Supplementary material associated with this article can be found, in the online version, at doi:10.1016/j.addlet.2023.100146.

APPENDIX A. Kinematic model of imperfect fabrication with homogenous transformation matrices

The accuracy model described in Section 4 uses a kinematic model of error stack-up to compute an imperfect Bend-Formed structure, given specified fabrication defects in feed length (δ_L), bend and rotate angle (δ_θ), and strut curvature (δ_κ). Here we describe the mathematical model for calculating the geometry of this imperfect structure, which consists of three steps:

1. Incorporate fabrication defects into the bend path of the perfect structure.
2. Model fabrication of the imperfect structure with homogenous transformation matrices (HTMs).
3. Add strut curvature to the imperfect geometry.

In the first step, we incorporate fabrication errors into the bend path of the perfect structure by adding the feed length error (δ_L) to each feed step and the angular error (δ_θ) to each bend/rotate step, such that a positive error corresponds to feeding, bending, and rotating more than required. If these errors are systematic, they are modeled as constant offsets to each fabrication step; if they are random, they are sampled from a normal distribution and vary for each fabrication step. The resulting imperfect bend path represents the fabrication instructions for the imperfect structure.

In the second step, we model the fabrication of the imperfect structure using homogenous transformation matrices (HTMs), which represent linear mappings of translation and rotation [27,28]. Following the coordinate system presented in Fig. 1, we model each feed step of the bend path as a translation along the y-axis, each bend step as a rotation about the negative z-axis and each rotate step as a rotation about the negative y-axis. Using these definitions, we calculate a homogenous transformation matrix for each line of the bend path. Then to calculate the nodes of the imperfect structure, we combine these matrices into N homogenous transformation matrices, where N is the number of feed steps in the bend path or equivalently the number of nodes in the geometry. We do this by multiplying together all matrices after each feed step, hence combining all fabrication steps after each node has been fed by the CNC wire bender. The resulting N matrices represent linear mappings from the origin (i.e. bend head of the machine) to nodes of the imperfect structure. By multiplying these N matrices to a list of N nodes at the origin, we obtain the geometry of an imperfect Bend-Formed structure. If no fabrication errors are present, this geometry is identical to the perfect Bend-Formed structure.

The final step is to add the strut curvature ($\delta_\kappa = \Delta/L$) to the imperfect geometry. We do this by fitting a symmetric, circular arc between the start and end points of each strut, using the maximum transverse offset Δ. The direction of this offset varies for each strut and is randomized by using by a random unit vector perpendicular to the strut axis. For a typical CNC wire bender, the direction of this offset may be controlled by the orientation of the feedstock spool; however, here we consider a purely random curvature direction.

These three steps allow the calculation of an imperfect Bend-Formed geometry with fabrication defects, as depicted in Fig. A1. With systematic fabrication defects, the kinematic model gives the same imperfect geometry each time, although the curvature direction for each strut is random. With random fabrication defects, the imperfect geometry varies each time, as dictated by the normal distributions of the errors.

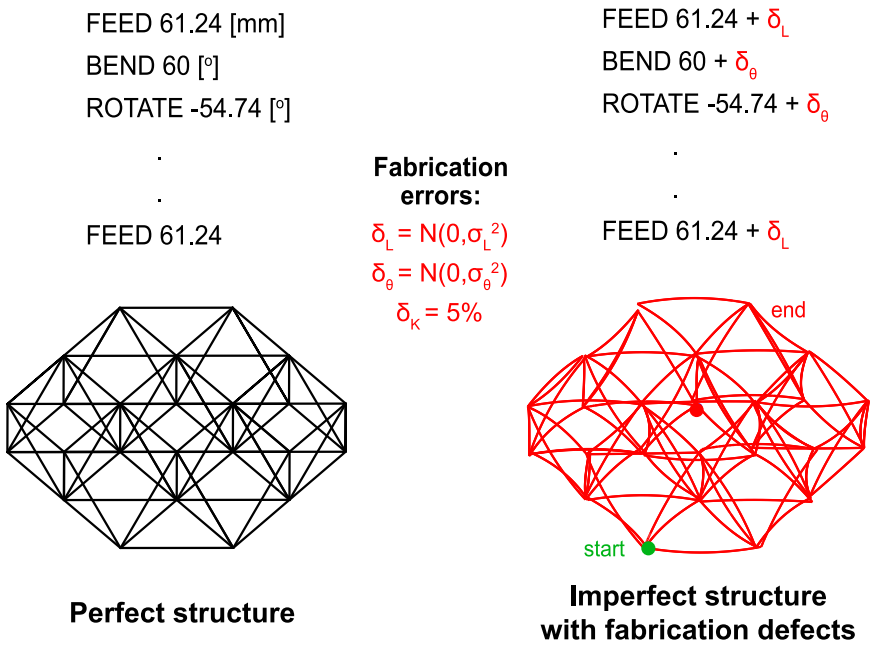

Fig. A1. Kinematic model of imperfect fabrication with Bend-Forming. Fabrication defects are incorporated into a perfect bend path and modeled via homogenous transformation matrices (HTMs) to calculate an imperfect geometry. The tetrahedral truss shown here has depth $H = 50$ mm and fabrication defects $[\sigma_L, \sigma_\theta, \delta_\kappa] = [0.2\text{ mm},\ 0.2°, 5\%]$.

References

[1] H.G. Bhundiya, F. Royer, Z. Cordero, Engineering framework for assessing materials and processes for in-space manufacturing, J. Mater. Eng. Perform. 31 (2) (2022), doi:10.1007/s11665-022-06755-y.

[2] D.Y. Yang, et al., Flexibility in metal forming, CIRP Ann. – Manuf. Technol. 67 (2) (2018) 743–765, doi:10.1016/j.cirp.2018.05.004.

[3] J.M. Allwood, H. Utsunomiya, A survey of flexible forming processes in Japan, Int. J. Mach. Tools Manuf. 46 (15) (2006) 1939–1960, doi:10.1016/j.ijmachtools.2006.01.034.

[4] A.A. El-Aty, et al., A review on flexibility of free bending forming technology for manufacturing thin-walled complex-shaped metallic tubes, Int. J. Lightweight Mater. Manuf. 6 (2) (2023) 165–188, doi:10.1016/j.ijlmm.2022.09.007.

[5] M. Strano, Automatic tooling design for rotary draw bending of tubes, Intern. J. Adv. Manuf. Technol. 26 (2005) 733–740, doi:10.1007/s00170-003-2055-6.

[6] Pensa Labs, D.I. Wire Pro. https://www.pensalabs.com/diwire-pro.

[7] M. Goodarzi, T. Kuboki, M. Murata, Deformation analysis of the shear bending process of circular tubes, J. Mater. Process. Technol. 162 (2005) 492–497, doi:10.1016/j.jmatprotec.2005.02.090.

[8] M. Murata, T. Kuboki, CNC tube forming method for manufacturing flexibly and 3-dimensionally bent tubes, 60 Excellent Inventions in Metal Forming, Springer Vieweg, Berlin, Heidelberg, 2015, doi:10.1007/978-3-662-46312-3_56.

[9] T. Kuboki, M. Furugen, S. Osaka, T. Ono, Development of die-less bending process for precision U-bent tube, in: Proceedings of *the 7th International Conference on Steel Rolling*, 1998, pp. 981–987.

[10] S. Chatti, M. Hermes, A.E. Tekkaya, M. Kleiner, The new TSS bending process: 3D bending of profiles with arbitrary cross-sections, CIRP Ann. 59 (1) (2010) 315–318, doi:10.1016/j.cirp.2010.03.017.

[11] R. Neugebauer, W.-.G. Drossel, U. Lorenz, N. Luetz, Hexabend – a new concept for 3D-freeform bending of tubes and profiles to preform hydroforming parts and end-form space-frame components, Adv. Technol. Plast. 2 (2023) 1465–1470.

[12] V. Holstein, M. Hermes, A.E. Tekkaya, Analysis of incremental die bending of wires and tubes, Prod. Eng. 14 (2020) 265–274, doi:10.1007/s11740-020-00952-1.

[13] N. Shimadaet, et al., Development of three-dimensional hot bending and direct quench technology, Procedia Eng. 81 (2014) 2267–2272, doi:10.1016/j.proeng.2014.10.319.

[14] D. Staupendahl, S. Chatti, A.E. Tekkaya, Closed-Loop control concept for kinematic 3D-profile bending, in: Proceedings of the AIP Conference, 2023, doi:10.1063/1.4963542.

[15] E. Miguel, M. Lepoutre, B. Bickel, Computational Design of Stable Planar-Rod Structures, ACM Trans. Graph. 35 (4) (2016) 1–11, doi:10.1145/2897824.2925978.

[16] H. Xu, E. Knoop, S. Coros, M. Bächer, Bend-It: design and fabrication of kinetic wire characters, ACM Trans. Graph. 37 (6) (2019) 1–15, doi:10.1145/3272127.3275089.

[17] V. Megaro, J. Zehnder, M. Bächer, S. Coros, M. Gross, B. Thomaszewski, A computational design tool for compliant mechanisms, ACM Trans. Graph. 36 (4) (2017) 1–12, doi:10.1145/3072959.3073636.

[18] R.A. Hamid, T. Ito, 3D prosthodontics wire bending mechanism with a linear segmentation algorithm, J. Adv. Manuf. Tech. (2016) 33–45 https://jamt.utem.edu.my/jamt/article/view/693.

[19] H.G. Bhundiya, "Bend-forming-algorithms," https://www.mathworks.com/matlabcentral/fileexchange/123360-bend-forming-algorithms.

[20] D. Jungnickel, Graphs, Networks and Algorithms, 4th ed., Spring Berlin Heidelberg, Germany, 2013, doi:10.1007/978-3-642-32278-5.

[21] G. Dreifus, et al., Path optimization along lattices in additive manufacturing using the chinese postman problem, 3D Print. Addit. Manuf. 4 (2) (2017) 98–104, doi:10.1089/3dp.2017.0007.

[22] J. Ebert, Computing Eulerian trials, Inf. Process. Lett. 28 (2) (1988) 93–97, doi:10.1016/0020-0190(88)90170-6.

[23] Van Sant Enterprises, Bend-tech pro tube bending software. https://www.trick-tools.com/Bend-Tech-Pro-Tube-Bending-Software-8147.

[24] R.A. Hamid, T. Ito, Integration of CAD/CAM in developing the CNC dental wire bending machine, JAMDSM 12 (3) (2018) 1–12, doi:10.1299/jamdsm.2018jamdsm0079.

[25] H.G. Bhundiya, F. Royer, Z. Cordero, Compressive behavior of isogrid columns fabricated with bend-forming, AIAA Scitech Forum, AIAA, San Diego, CA & Virtual, 2022 January 3-72022, doi:10.2514/6.2022-2263.

[26] FormLabs, "Form 3," https://formlabs.com/3d-printers/form-3/.

[27] KabelMat, Winding, measuring & warehouse systems – complete catalogue. https://www.helukabel.se/HELUKABEL/Sweden/kabelmat_catalog_en.pdf.

[28] B. Siciliano, O. Khatib (Eds.), Springer Handbook of Robotics, Springer-Verlag Berlin Heidelberg, Germany, 2008, doi:10.1007/978-3-540-30301-5.

[29] A.H. Slocum, Precision Machine Design, Prentice Hall, Englewood Cliffs, NJ, 1992.

[30] K. Miura, S. Pellegrino, Forms and Concepts for Lightweight Structures, Cambridge University Press, Cambridge, 2020, doi:10.1017/9781139048569.

[31] W.H. Greene, Effects of random member length errors on the accuracy and internal loads of truss antennas, J. Spacecr. Rocket. 22 (5) (1985) 554–559, doi:10.2514/3.25065.

[32] M.M. Mikulas, H.G. Bush, and M.F. Card, "*Structural stiffness, strength and dynamics characteristics of large tetrahedral space truss structures*," 1977, NASA Technical Memorandum X-74001.

[33] J.M. Hedgepeth, Influence of fabrication tolerances on the surface accuracy of large antenna structures, AIAA J. 20 (5) (1982) 680–686, doi:10.2514/3.7936.

[34] J. Hedgepeth, Primary design requirements for large space structures, in: Proceedings of the *2nd AIAA Conference on Large Space Planforms*, AIAA, San Diego, CA, 1981 February 2-4, 1981, doi:10.2514/6.1981-443.

[35] M.S. Lake and N. Georgiadis, "*Analysis and testing of axial compression in imperfect slender truss struts*," 1990, NASA Tech. Memo. 4174.

[36] K.C. Wu and M.S. Lake, "*Natural frequency of uniform and optimized tetrahedral truss platforms,*" 1994, NASA Technical Paper 3461.

[37] H.G. Bush, et al., Design and fabrication of an erectable truss for precision segmented reflector application, J. Spacecr. Rocket. 28 (2) (1991) 251–257, doi:10.2514/3.26238.